Reformate Gas Composition and Pressure Effect on CO Tolerant Pt/Ti$_{0.8}$Mo$_{0.2}$O$_2$-C Electrocatalyst for PEM Fuel Cells

M. Suha Yazici, Sümeyye Dursun, Irina Borbath, András Tompos

Reformate Gas Composition and Pressure Effect on CO Tolerant Pt/Ti$_{0.8}$Mo$_{0.2}$O$_{2}$-C Electrocatalyst for PEM Fuel Cells

M. Suha Yazici*[,1], Sümeyye Dursun[2], Irina Borbath[3], András Tompos[3]

1. TUBITAK Marmara Research Centre, Energy Institute, Gebze-Turkey

2. Department of Chemical Engineering, Kocaeli University, Kocaeli-Turkey

3. Institute of Materials and Environmental Chemistry, Research Centre for Natural Sciences,

H-1117 Budapest, Magyar tudósok körútja 2, Hungary

*Corresponding author: e-mail: suha.yazici@tubitak.gov.tr

Abstract

Mixed-oxide coated Ti$_{0.8}$Mo$_{0.2}$O$_{2}$–C composite supported 20 wt.% Pt electrocatalysts with Ti$_{0.8}$Mo$_{0.2}$O$_{2}$/C= 75/25 mass ratio were developed for CO tolerance of polymer electrolyte membrane fuel cell (PEMFC) anode. Studies of the structure, composition and stability, as well as the results of CO$_{ads}$ stripping confirmed that the mixed oxide composite support and the electrocatalyst prepared for this study show the well-documented characteristics of the Pt/Ti$_{1-x}$Mo$_{x}$O$_{2}$-C systems and Pt/Ti$_{0.8}$Mo$_{0.2}$O$_{2}$-C catalyst with enhanced CO tolerance compared to the Pt/C catalyst is suitable for further investigation as an anode in reformate-fed PEMFCs.

Dilution of hydrogen with CO$_{2}$ and CH$_{4}$ had negligible negative impact on the fuel cell performance. Switching gas composition between hydrogen and reformate shows recovery of potential after CO poisoning. Nevertheless, anode catalyst loading of 0.25 and 0.5 mgPt/cm^{2} was not enough to give reasonable performance when CO impurity was present. Loading of 0.85 mgPt/cm^{2} Ti$_{0.8}$Mo$_{0.2}$O$_{2}$–C supported catalyst was effective to give 1000 mA/cm^{2} current density at 0.6 V under 25 ppm CO and 30 psig. Higher loading was needed at mass transfer limited region to overcome poisoning. However, loadings higher than 0.85 mgPt/cm^{2} caused mass transfer limitations. Hence higher loadings is proposed with 40 wt.% Pt/Ti$_{0.8}$Mo$_{0.2}$O$_{2}$-C support catalyst.

Keywords: Composite materials, Pt electrocatalyst, reformate, CO tolerance, fuel cell

Highlights

- Ti$_{0.8}$Mo$_{0.2}$O$_{2}$–C supported Pt electrocatalysts were developed for CO tolerance
- 20 % Pt/ Ti$_{0.8}$Mo$_{0.2}$O$_{2}$-C catalyst showed good stability over 500 cycles
- Loading of 0.85 mgPt/cm^{2} was effective to give 1000 mA/cm^{2} at 0.6 V under 25 ppm CO
- Reformate with CO$_{2}$ and CH$_{4}$ show impact of hydrogen dilution at mass transfer region

Introduction

For wide-range applications of Polymer Electrolyte Membrane Fuel Cell (PEMFC) based combined heat and power (CHP) systems, it is necessary to utilize low-cost catalyst with long-term durability. Pt-based anode electrocatalysts that are used in PEMFC systems are easily poisoned by a small amount of CO, present in reformate gases, leading to performance losses and reduced lifetime. Adsorption of CO on metal catalyst surface prevents reaction of hydrogen, resulting anode polarization and performance losses.

Pt-Ru/C catalysts are used as anode catalyst for reformate fuel to eliminate detrimental CO effect on Pt catalyst [1-2]. Unstable nature of PtRu alloy leads to dissolution of Ru under reformate-fed PEM fuel cell operating conditions leading to reduced lifetime. Highly stable electrocatalysts with long life, low cost and better electrochemical activity along with decreased Pt content are needed to replace commercially used PtRu anode catalyst. Presence of not only CO but also CO_2 in reformate-fed fuel cell was investigated for electrocatalysts using Pt, Pt/Ru (1:1) and supported Pt:Mo electrocatalysts with various atomic ratios. Interestingly, presence of CO_2 resulted in reduction of the overpotential over PtRu/C (1:1) while similar overpotential for Pt/C and PtMo/C (5:1) were reported [3].

Mixed oxides as support for electrocatalysts with increased stability were tried by different researchers [4-7]. $Pt/Ti_{0.7}W_{0.3}O_2$ electrocatalyst was reported to have low potential electrooxidation of CO (below 0.1 V) similarly to porous Pt electrodes with adsorbed W species and Mo-modified Pt single-crystal electrodes [8-10]. H_2 oxidation in the presence of 2 % CO for Pt/C, PtRu/C, and $Pt/Ti_{0.7}W_{0.3}O_2$ catalysts showed $Pt/Ti_{0.7}W_{0.3}O_2$ give lowest onset potential for H_2 oxidation (0.05 V vs RHE) relative to both Pt/C and PtRu/C (0.250 V vs RHE) [11].

Molybdenum (Mo) was utilized for CO-tolerant electrocatalyst due to relatively low cost and good catalytic activity of PtMo alloy [12-13]. Mo provides necessary OH_{ad} species for the electrooxidation of CO_{ad} at less positive potentials than Pt (according to "bifunctional mechanism") [14]. The effectiveness of the $MoO_x@Pt$ core-shell and well-defined $Pt_{0.8}Mo_{0.2}$ alloy electrocatalysts for higher CO tolerance and durability was demonstrated by Hu *et al*. [15]. It was shown that Mo species was critically important for hydrogen oxidation and CO tolerance. However, Mo is easily oxidized at low potentials and has low electronic conductivity. Moreover, single molybdenum oxides are readily dissolved under operating conditions of the PEM fuel cell unless it is incorporated into the TiO_2-rutile lattice.

Recently, combination of TiO_2 with MoO_x, was shown to have good conductivity and relative stability in acid solutions [16-17]. TiO_2 was stable in acid electrolyte [18]. TiO_2 also helps stabilizing metals in highly dispersed state, essential to control catalyst nanostructure, thermal and oxidation stability. However, TiO_2 has low electronic conductivity.

Mixed-oxide coated $Ti_{0.8}Mo_{0.2}O_2$–C composites with Ti/Mo= 80/20 atomic ratio was used as an optimal composition because of complete Mo incorporation into the rutile lattice providing high stability in the anticipated pH/potential window [19]. Better CO tolerance and increased electrocatalytic stability of 20 wt.% $Pt/Ti_{0.8}Mo_{0.2}O_2$-C electrocatalyst compared to the commercial PtRu/C (Quintech) catalyst was demonstrated [20]. The catalytic properties of the Mo-doped TiO_2–carbon composite supported Pt catalysts were mainly determined by the interactions between Mo and Pt.

The concept of Mo-doped TiO_2–carbon composite support was based on the idea of bringing together excellent stability and nanoparticle-stabilizing ability of TiO_2 with good co-catalytic properties of Mo and with good conductivity and large surface area of carbonaceous materials in a unique material system [21-22]. If stability of composite supported Pt catalyst is indeed improved with respect to the Pt/C system, there is significant room for decreasing the Pt content. The electrochemical studies of the Mo-containing composite supported Pt catalysts were completed by model studies during which Mo was electrochemically deposited onto Pt electrodes [23]. It has been demonstrated by XPS measurements that the sites of the catalysts responsible for CO tolerance are formed in the interfaces of Pt particles and reducible Mo species.

Present research investigates impact of catalyst loading, pressure and gas composition on PEM fuel cell performance of mixed-oxide coated $Ti_{0.8}Mo_{0.2}O_2$–C composite supported Pt anode catalyst. Different reforming processes produces hydrogen-rich reformate gases different in compositions which usually contains 15-35 % carbon dioxide (CO_2) and nitrogen (N_2), some methane (CH_4) and about 40 % hydrogen (H_2) with ppm level carbon monoxide [24]. Reformate with and without CO were tried to understand effect of dilution with CO_2 and CH_4. Test under pure hydrogen was used to evaluate poisoning and mass transfer impact of reformate in continuous cycles.

Experimental

Synthesis of $Ti_{0.8}Mo_{0.2}O_2$-C composite materials and Pt electrocatalysts
$Ti_{0.8}Mo_{0.2}O_2$ mixed oxide and high surface area carbon (CABOT, Black Pearls 2000) composite support materials (1 g) were prepared by multistep sol-gel synthesis according to our previous studies [19-20]. Preparation of the $Ti_{0.8}Mo_{0.2}O_2$-C composite materials with $Ti_{0.8}Mo_{0.2}O_2$/C= 75/25 wt.% content is schematically shown in Figure 1. The nominal composition of the investigated composite support with atomic ratio Ti/Mo= 80/20 was $Ti_{0.8}Mo_{0.2}O_2$-C. Electrocatalysts containing nominally 20 wt.% of Pt were deposited on the composite support using $NaBH_4$-ethylene glycol reduction-precipitation method as described in details in Refs. [19-20]. The appropriate amount of electrocatalyst have been obtained in four batches. Characterization of different batches of the $Pt/Ti_{0.8}Mo_{0.2}O_2$-C electrocatalysts was done before unifying them. The results show good reproducibility of the synthesis.

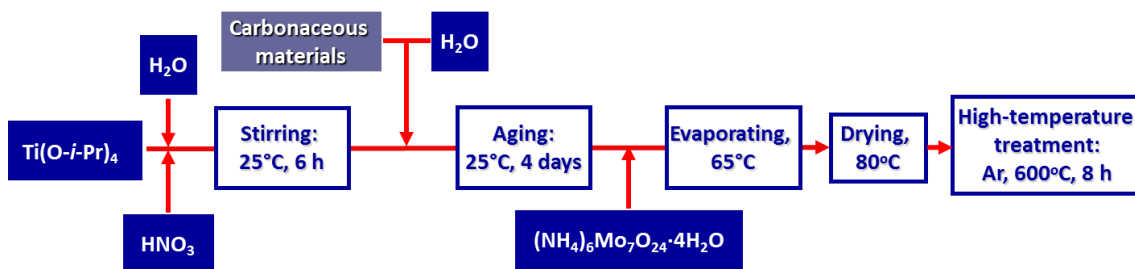**Figure 1.** Preparation steps of $Ti_{0.8}Mo_{0.2}O_2$-C composite materials.

Physical characterization

X-ray diffraction (XRD), transmission electron microscopy (TEM) and scanning electron microscopy (SEM) analysis were performed to characterize structure and surface of the electrodes. Philips model PW 3710 based PW 1050 Bragg-Brentano parafocusing goniometer using CuK_α radiation (λ= 0.15418 nm), graphite monochromator and proportional counter was used to obtain XRD patterns. TEM-JEOL 2100 HRTEM transmission electron microscope was utilized to acquire high-resolution images of the samples. The average diameter and particles size were calculated utilizing at least ten micrographs of each sample by measuring the diameters of no less than 1000 randomly selected metal particles. Scanning electron microscopy (SEM - JSM6335-F Oxford Instruments AZTEC-EDS) used to look at cross-section of the MEA.

Electrochemical characterization

Standard three-electrode configuration was used for electrochemical measurements using 0.5 M H_2SO_4 as electrolyte. Glassy carbon with 0.0707 cm^2 surface area was used as working electrode, while platinum wire was used as counter electrode and a hydrogen electrode, immersed in the same electrolyte as reference electrode. Details on the preparation of working electrode and catalyst ink composition were described in Refs. [19-21].

Conditioning of the electrocatalysts before cycling voltammetry (CV) measurements and three-step electrochemical experiments consisted of (i) the CO_{ads}-stripping voltammetry measurement, (ii) 500 polarization cycles for stability test and (iii) the second CO_{ads}-stripping voltammetry measurement were routinely applied according to our previous studies [20]. Potentials are given vs. RHE.

The Q_{H-UPD} charges, associated with hydrogen adsorption/desorption, were calculated using conventional baseline correction. The loss in electrochemically active Pt surface area (Δ ECSA) upon stability tests was calculated from the charges originated from the hydrogen desorption in the 1st and 500th cycles (Equation 1):

$$\Delta ECSA_H = \{1-(ECSA_{500}/ECSA_1)\} \times 100\% \quad\quad\quad \text{(Equation 1)}$$

After every stability test the electrolyte was changed to fresh one to avoid the re-deposition of the dissolved metals. Electrochemical performance of the $Pt/Ti_{0.8}Mo_{0.2}O_2$-C electrocatalyst was compared with 20 wt.% Pt/C (Quintech) commercial catalyst.

Electrochemical single fuel cell measurements

Single cell hardware with 5 cm^2 active area was used for fuel cell measurements. Cathode was loaded with 0.6 mg/cm^2 Pt (20 wt.% Pt/C) and anode with 0.25, 0.5 and 0.85 mg/cm^2 Pt (20 wt.% Pt/Ti$_{0.8}$Mo$_{0.2}$O$_2$-C) onto Sigracet 29BC GDL by painting. Nafion XL membrane was first boiled in 3 wt.% H$_2$O$_2$ solution, then, 0.5 M H$_2$SO$_4$, and finally in water for 1 h. Treated membrane and catalyst loaded GDLs were used to make MEAs for fuel cell testing by hot pressing at 100 °C under pressure of 30 kg cm^{-2} for 5 min. Polarization measurements were taking first under hydrogen gas, then, with reformate gas (25 ppm CO, 16 % CO$_2$, 8 % CH$_4$, 42 % H$_2$, 34 % N$_2$) with and without CO. Cathode side was fed with oxygen in all cases. Single cell was conditioned at least 8 hours and operated under different pressures (0 to 30 psig), temperature (80 $^{\circ}$C) and gas conditions (hydrogen, reformate with and without CO).

Results and discussion

Characterization of the Ti$_{0.8}$Mo$_{0.2}$O$_2$-C composite materials and related Pt catalysts
The preparation procedure of the Ti$_{0.8}$Mo$_{0.2}$O$_2$-C composites and related Pt catalysts was supervised by X-ray diffraction. According to our previous studies [19-20], XRD measurements gave information about the phase composition of the samples (rutile and/or anatase TiO$_2$, presence or absence segregated MoO$_x$ phase). In addition, taking into account the fact that Mo-incorporation resulted in a characteristic distortion of the rutile-TiO$_2$ cell and the change in the cell parameters was proportional to the extent of the molybdenum incorporation into TiO$_2$ phase, the incorporation rate could also be quantified [19]. It has been demonstrated that the incorporation of Mo in the presence of carbon was much more effective in case of rutile TiO$_2$ than in case of anatase [19, 22]. After the multistep sol-gel synthesis procedure and high-temperature treatment (HTT), the success of the synthesis of Mo-doped composites with appropriate structure was verified by X-ray diffraction measurements. According to the results of XRD experiments in composite materials before and after HTT at 600 °C for 8 hours in argon flow, only the reflections of the TiO$_2$-rutile crystallites were observed (Figure 2, samples 1 and 2, respectively); no reflections characteristic to Mo oxides were found. The characteristic distortion in the lattice parameters of the rutile phase obtained after HTT (a= 4.640 Å, c= 2.935 Å; pure rutile TiO$_2$: a= 4.593 Å, c= 2.959 Å) confirmed the incorporation of Mo into TiO$_2$-rutile lattice with Mo$_{subst}$= 21 % [19]. It is necessary to mention that exclusive incorporation of Mo ions into substitutional sites of the TiO$_2$, guaranteeing high stability across the anticipated potential/pH window of an operating PEM fuel cell. In this case, TiO$_2$ lattice protected molybdenum from dissolution while Mo incorporated into Ti$_{(1-x)}$Mo$_x$O$_2$ mixed oxide could still provide CO tolerance and enhanced electronic conductivity [19-20]. Pt loading resulted in the appearance of the reflections characteristic to the diffraction planes (111), (200), and (220) of the fcc structure of Pt at 2 theta values of 39.6, 47.4, 67.1°, respectively [25, 26] (Figure 2, sample 3). The broad line profile of Pt corresponds to very small crystallites. It is necessary to mention that Pt loading does not affect the reflections of the TiO$_2$-rutile phase. The observed structural characteristics were in

a good agreement with those found in our earlier studies, indicating the high reproducibility of the synthesis [19, 20, 22].
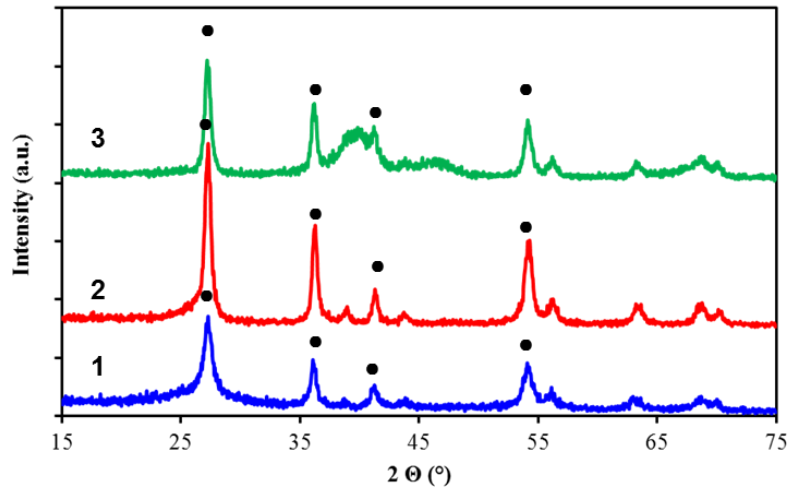

Figure 2. XRD patterns of $Ti_{0.8}Mo_{0.2}O_2$-C composites before HTT (sample 1), after HTT in Ar (sample 2) and after Pt loading (sample 3). ●- Rutile.

In accordance with our previous studies [19-20] the presence of the Pt nanoparticles with mean particle size of about 2.9 nm and narrow distribution (± 0.8 nm) was observed by TEM at different magnifications (Figure 3a-c). As shown in Figures 3a-c, the dark spots assigned to the Pt particles are rather uniformly present in the micrographs.

Moiré patterns observed in Figure 3b emerged from overlapping slightly misaligned crystallites of mixed oxide on the top of each other. The widespread appearance of these patterns indicated that quite homogeneous oxide coverage over carbon was achieved. It was important as the contrast between the carbon and the mixed oxide was generally low and their distinction was difficult. Moreover, in our previous studies [19-20] it was shown that the presence of a few large, nanorod-like mixed oxide rutile crystallites were general feature of composites with a high content of mixed oxides ($Ti_{0.8}Mo_{0.2}O_2$/C= 75/25). Figure 3d shows cross-section of the membrane electrode assembly (MEA) cut by freezing for cross-sectional analysis. Membrane with 25 micron thickness was surrounded with approximately 25 micron anode (1.54 mgPt/cm^2 loading) thickness and 10 micron cathode (0.6 mgPt/cm^2 loading) thickness.
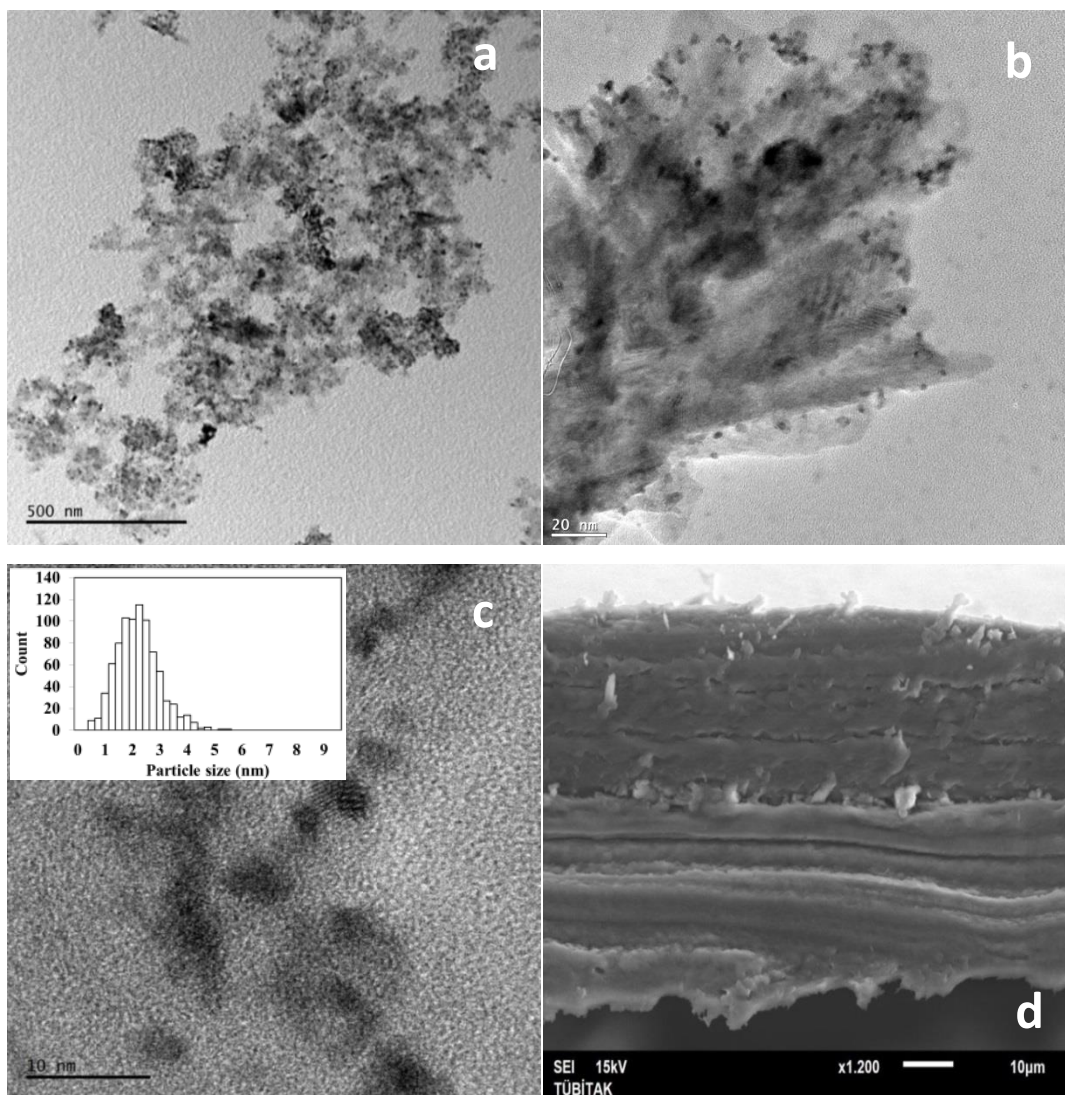
Figure 3. TEM images and histogram of the distribution of particle size at 500 nm (a), 20 nm (b) and 10 nm (c) for the 20 wt.% $Pt/Ti_{0.8}Mo_{0.2}O_2$-C electrocatalyst and cross-section of the membrane electrode assembly (MEA) with 1.54 mgPt/cm^2 loading measured by SEM (d).

Cyclic voltammograms of the 20 wt.% $Pt/Ti_{0.8}Mo_{0.2}O_2$-C and commercial 20 wt.% Pt/C (Quintech) electrocatalysts obtained on fresh samples and after 500-cycle stability test were presented on Figure 4a. As shown in Figure 4a on the $Ti_{0.8}Mo_{0.2}O_2$-C composite supported Pt catalyst besides the classical features of the under-potentially deposited hydrogen adsorption/desorption between 50 mV and 350 mV, a characteristic redox peak pair between 380 mV and 530 mV, which was assigned to oxidation/reduction of reducible MoO_x surface species, were also detected.
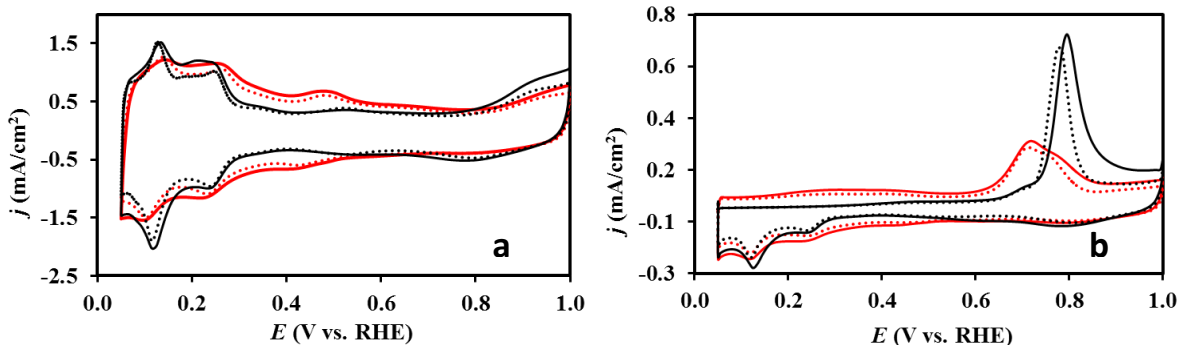
Figure 4. CVs (a) and CO_{ads} stripping voltammograms (b) of the $Pt/Ti_{0.8}Mo_{0.2}O_2$-C (red) and the Pt/C (black) catalysts obtained on fresh catalysts (solid lines) and after stability test (dotted lines) in 0.5 M H_2SO_4. Pt loading of the electrodes was 10 µg/cm^2. Sweep rate: (a) 100 mV/s (a) and (b) 10 mV/s, T= 25 ^{o}C.

As an analogy with literature [27, 28] the presence of these Mo redox peaks in the voltammograms of the $Ti_{(1-x)}Mo_xO_2$–C composite supported Pt electrocatalysts, confirming the presence of an active interface between the Pt nanoparticles (NPs) and Mo-containing support, has already been demonstrated in our earlier studies [19-23]. Moreover, in acidic solutions the redox peak pair observed in the Mo-containing Pt catalysts can also be interpreted as the formation/decomposition of molybdenum bronze species by the "spillover" of hydrogen between Pt and Mo surface sites [29-31]. It is necessary to mention that the intercalation of hydrogen into the MoO_3 lattice is accompanied by reduction of the metal ions and formation of H_xMoO_3 with Mo in mixed valent state (5+/6+) [32].

As shown on Figure 4b the CO electrooxidation on the $Pt/Ti_{0.8}Mo_{0.2}O_2$-C catalyst starts at ca. 50 mV. Due to providing adsorbed hydroxyl species (OH_{ads}) for CO oxidation at very low electrode potentials [33, 34] this behavior of the Mo-containing composite supported Pt catalysts is not surprising and was already demonstrated in our earlier studies [19-23]. The presence of a characteristic "pre-peak" between 150 and 550 mV and the shift to less positive potentials of the position of the main CO oxidation peak observed on the $Pt/Ti_{0.8}Mo_{0.2}O_2$-C catalyst in comparison to that on Pt/C (715 mV and 800 mV, respectively) also indicated the CO-tolerant behavior of composite supported catalyst.

For the practical application of anode catalysts in fuel cells, leaching of non-noble components can cause decrease in CO tolerance and deterioration of membrane [35,36]. As shown in Figure 4a during the electrochemical stability tests for 500 polarization cycles very small performance loss was observed on the $Pt/Ti_{0.8}Mo_{0.2}O_2$-C and the reference commercial Pt/C catalysts. The electrochemically active Pt surface area of the $Pt/Ti_{0.8}Mo_{0.2}O_2$-C and Pt/C electrocatalysts calculated from the CVs was 72.1 m^2/g$_{Pt}$ and 94.5 m^2/g$_{Pt}$, respectively. After 500 cycles, the loss in ECSA (Δ ECSA$_H$) on the $Pt/Ti_{0.8}Mo_{0.2}O_2$-C and Pt/C, calculated according to Equation 1, was 6.6 % and 12.7 %, respectively. Similar results of the 500-cycle stability test done by potential

cycling between 0.05 and 1.1 V were obtained in Ref. [11] on 5 wt.% $Pt/Ti_{0.7}W_{0.3}O_2$ catalyst mixed with 20 wt.% C carbon powder; after 500 cycles, the decrease of the Q_{H-UPD} over $Pt/Ti_{0.7}W_{0.3}O_2$ electrocatalyst was 5 %.

In our previous publication [20] the comparison between the electrocatalytic behavior of the state-of-art commercial CO-tolerant PtRu/C (Quintech) and the $Pt/Ti_{0.8}Mo_{0.2}O_2$-C systems has been described. It is well known that oxophilic metal-containing catalysts become unstable at high potentials [37]. Therefore, to avoid strong surface oxidation and irreversible damage of the structure of the Ru-containing electrocatalyst, the upper potential used was limited to 1.0 V.

It has been found that 500-cycle stability test, performed using these polarization conditions, results in serious degradation of the reference PtRu/C; the $\Delta ECSA_{CO}$ calculated from the 1st and 2nd CO-stripping measurements (details see in Ref. [20]) was ca. 20 % and 55 % for $Pt/Ti_{0.8}Mo_{0.2}O_2$-C and PtRu/C catalysts, respectively.

Thus, according to the literature [6, 38-40] and our previous results [19-22], the role of the oxide in the composite material is to stabilize the Pt content of the catalyst in a highly dispersed state. If a significant part of the Pt content is in direct contact with the oxide component of the composite, it can still exert its stabilizing effect on the Pt particles, even if the carbon becomes partially corroded. On the other hand, the CO tolerance also requires very intimate contact between the Mo-containing oxide and the Pt. Thus, the surface electrochemistry of the catalysts is largely determined by the Pt-Mo interfacial sites, which are probably less in composites with lower mixed oxide to carbon mass ratio ($Ti_{0.8}Mo_{0.2}O_2$/C= 50/50 or 25/75).

However, the too high mixed oxide content ($Ti_{0.8}Mo_{0.2}O_2$/C= 75/25) beneficial for improved CO tolerance, can result in a lower electrical conductivity, due to the presence of thick oxide layer with higher resistance in comparison to carbon. Therefore, in this study, we tried to compensate possible negative effect of high oxide content by using commercial Black Pearls 2000 with a large specific surface area (S_{BET}= 1502 m^2/g) as carbon component for the preparation of composite materials. Moreover, upon the synthesis of the composite materials the preparation conditions used (long aging time at room temperature (see Figure 1)) favored the nucleation and growth of the rutile-TiO_2 oxide coatings over the carbonaceous backbone. Thus, studies of the structure, composition and stability, as well as the results of CO_{ads} stripping confirmed that the mixed oxide composite support and the electrocatalyst prepared for this study show the well-documented characteristics of the $Pt/Ti_{1-x}Mo_xO_2$-C systems and $Pt/Ti_{0.8}Mo_{0.2}O_2$-C catalyst with $Ti_{0.8}Mo_{0.2}O_2$/C=75/25 mass ratio is suitable for further investigation as an anode in reformate-fed PEM fuel cells.

Characterization in a single PEM fuel cell
Figure 5 shows current-time profile under 0.5 V polarization under different gas compositions and flow rates. Following conditioning for 8 hours under hydrogen flow, cell was pressurized to 5 psi overpressure and operated at 80 ^{o}C. Cell performance was increased giving 6 A current at

0.5 V. When reformate gas with CO (25 ppm CO, 16 % CO_2, 8 % CH_4, 42 % H_2, 34 % N_2) was fed into the cell, current, under same voltage polarization, fell about 50% to 3 A. Since amount of hydrogen in the reformate was low, different flow rates (0.2-0.5 l/min) were tried to account for mass transfer effect in the current generation. There was no significant change at current (3 A at 0.5 V polarization) with increasing flow rate of reformate gas. Switching gases between hydrogen and reformate was able to give previous current values indicating CO surface coverage was not irreversible. After 3.5 hours, gas switched back to hydrogen. Current reached above 7 A within 1 hour after back pressure was increased from 5 psi to 30 psi for hydrogen. When gas was switched back to reformate with 25 ppm CO, current settled around 4.75 A. This was about 60 % higher than the current values at 5-psi back pressure. Polarization curves indicated catalyst was performing well with 25 ppm CO, especially at higher cell backpressures.
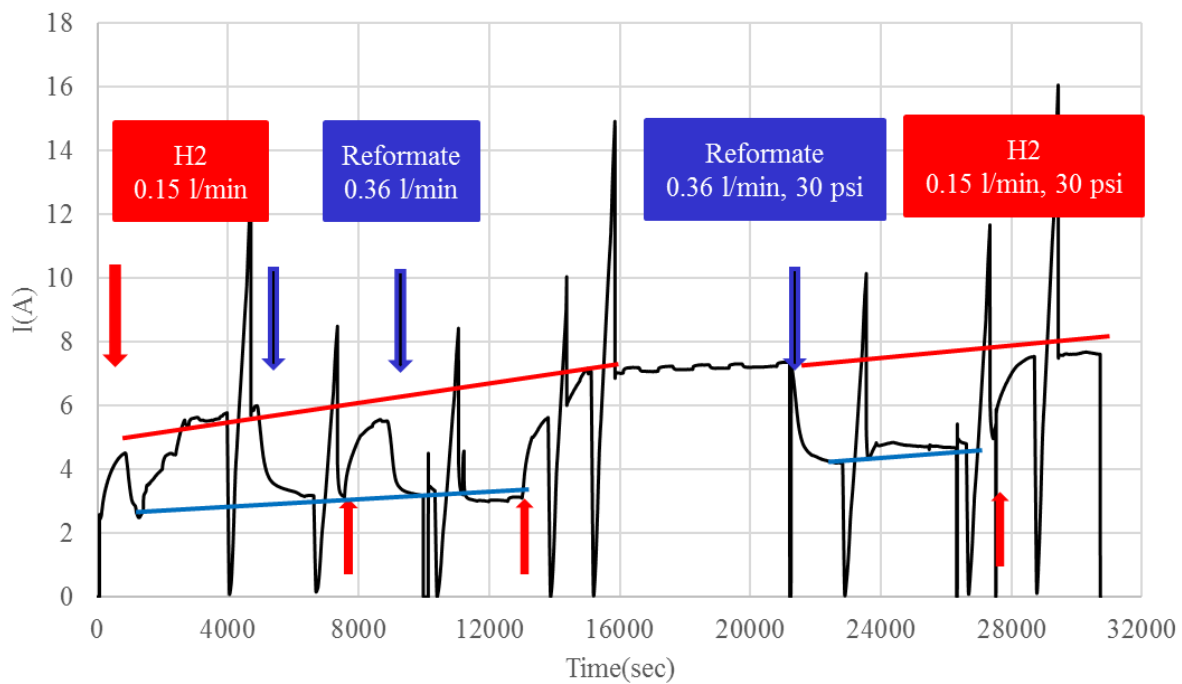

Figure 5. Change of current with time under 0.5 V polarization for 5 cm^2 single-cell with 0.85 mgPt/cm^2 loaded Pt/Ti$_{0.8}$Mo$_{0.2}$O$_2$-C anode. Cell temperature: 80 ^{o}C, 100 % RH.

Current variations under different temperatures and different voltage polarizations (0.7 V, 0.6 V and 0.5 V) were observed for reformate containing 25 ppm CO (Figure 6). Polarization under hydrogen was compared to reformate with and without CO to distinguish between CO, CO_2 and mass transfer effect due to hydrogen dilution. Reformate with no-CO showed about 250 mA lower current than pure hydrogen at kinetic and ohmic regions (Figure 6a). Performance and CO tolerance of the cell was improved when reformate temperature was increased from 60 ^{o}C to 90 ^{o}C. When cell was polarized to mass transfer region (0.5 V), there was no difference between pure hydrogen and reformate with no-CO (Figure 6b). Gas dilution, compensated with higher

flow rate, showed its effect above 1000 mA/cm^2 current density causing mass transfer limited performance drop compare to hydrogen. When reformates with and without CO was compared, there was less than 200 mV voltage drop at 1000 mA/cm^2 current density.
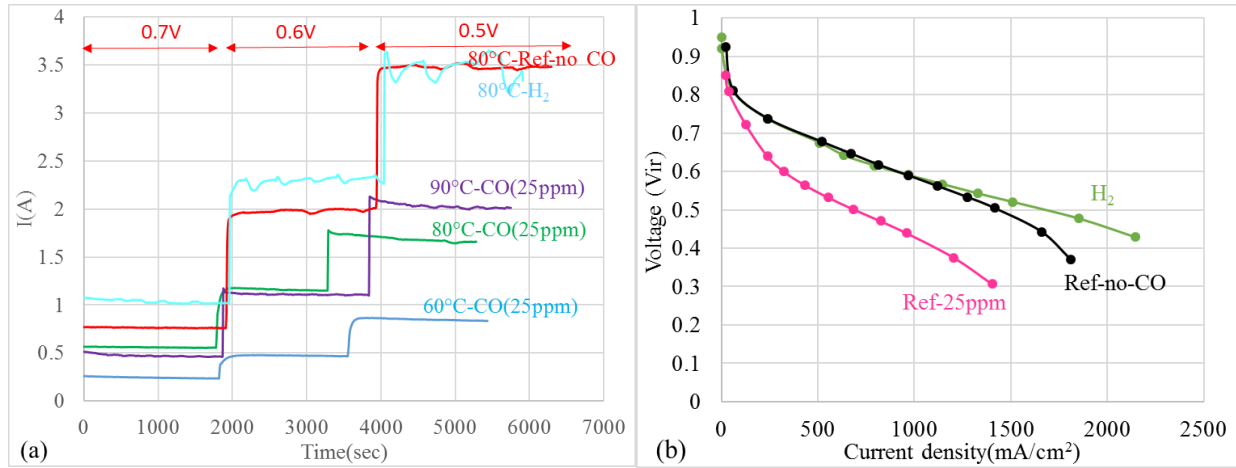

Figure 6. Time (a) and polarization (b) responses for 0.85 mg Pt/cm^2 loaded Pt/Ti$_{0.8}$Mo$_{0.2}$O$_2$-C anode under hydrogen and reformate. Cell temperature 80 ^{o}C, RH 100 % and 5-psi back pressure.

Catalyst Loading

Various Pt loading of 20 wt.% Pt/Ti$_{0.8}$Mo$_{0.2}$O$_2$-C was compared for performance in Figure 7. Anode Pt loadings of 0.25, 0.5 and 0.85 mgPt/cm^2 were given similar polarization response under pure hydrogen gas (Figure 7a). This was in agreement with literature that hydrogen side kinetics was good even under 0.2 mgPt/cm^2 loading. When same catalysts were subjected to reformate gas with 25 ppm CO, performance differences were clearly observed (Figure 7b). Loading of 0.25 mgPt/cm^2 was not enough to reach current densities above 1000 mA/cm^2. Polarization response at kinetic region was similar for both 0.5 and 0.85 mgPt/cm^2 loaded electrodes. Higher Pt loading gave better ohmic and mass transfer response as current density increased since cleaner Pt surface was available for oxidation reaction to take place under same flow rate and current density. Effect of Pt loading on maximum current density at different voltage levels was shown in Figure 7c. Loading of 0.25 mgPt/cm^2 have resulted less than 50 mA variation between 0.7 V and 0.5 V polarizations. Highest variation was 500 mA current difference between 0.7 V and 0.5 V with 0.85 mgPt/cm^2 loading. After 10 days of operation, current densities at different voltage levels were much lower as marked with dots on Figure 7c. Figure 7d shows mass activity for different Pt loading with reformate (25 ppm CO) gas. Mass activity was better for low loading at kinetically limited region. Higher loading was needed at mass transfer limited region to overcome poisoning.
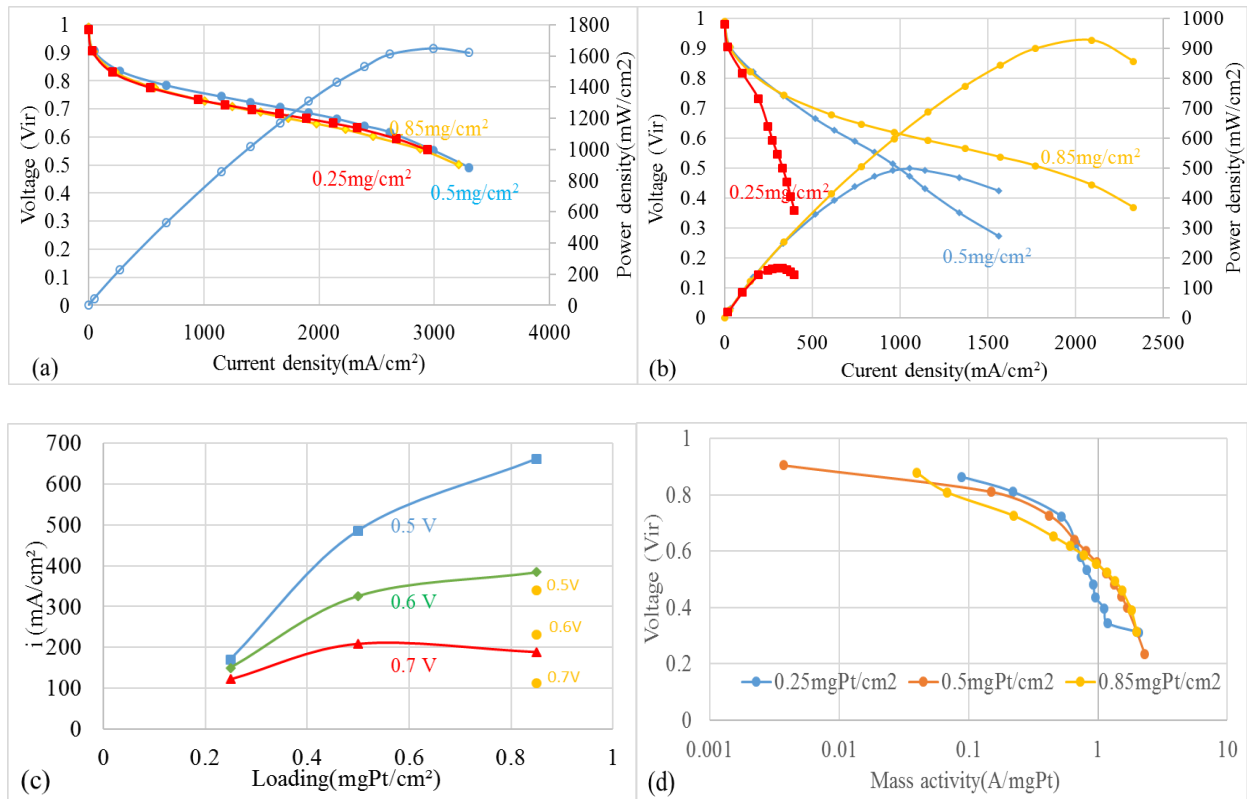
Figure 7. Polarization responses for different loading of anode under hydrogen (a) and 25 ppm reformate-fed CO (b). Effect of different loadings on current (c) and mass activity (d) with 25 ppm reformate-fed CO. Cell temperature 80 ^{o}C, RH: 100 % and 30-psi back-pressure.

Pressure Effect

Effect of cell pressure on the performance of 20 wt.% Pt/Ti$_{0.8}$Mo$_{0.2}$O$_2$-C anode catalyst with 0.85 mgPt/cm^2 loading is shown in Figure 8. Reformate diluted hydrogen without CO had better performance than reformate with CO (Figure 8a-b). Higher pressure was very effective with reformate for higher performance. Close to 100 mV voltage improvement was measured at 1000 mA/cm^2 current density going from 5 psi to 30-psi pressure (Figure 8b). As shown in Figure 8c, performance increase for 0.85 mgPt/cm^2 loading was significant compare to other loadings when fuel cell pressure was increased from 5 psi to 30 psi. Similarly, mass activity was better under high pressure for kinetic, ohmic and mass transfer regions (Figure 8d).
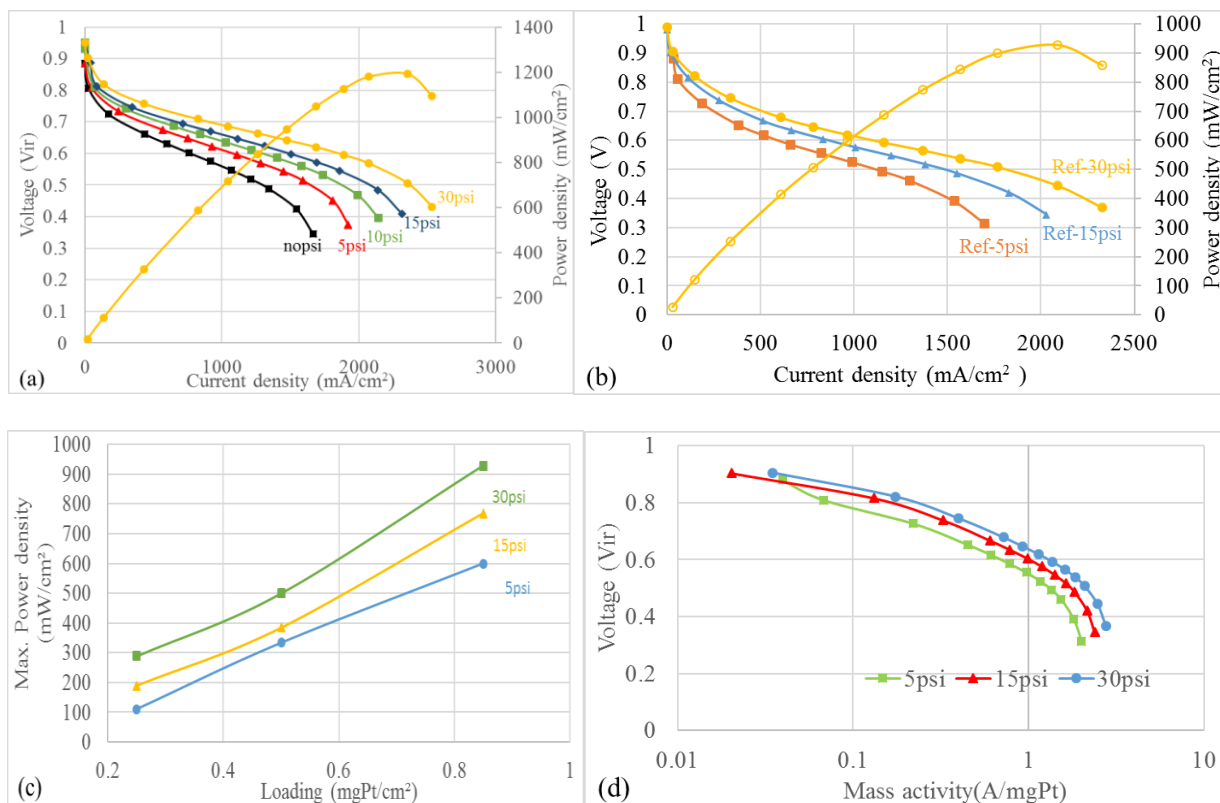
Figure 8. Back pressure effect on 0.85 mg Pt/cm^2 loaded Pt/Ti$_{0.8}$Mo$_{0.2}$O$_2$-C anode with no CO-reformate (a), Reformate with 25-ppm CO (b), power density at different loadings (c) and mass activity (d).

Conclusions

20 wt.% Pt/Ti$_{0.8}$Mo$_{0.2}$O$_2$-C with Ti$_{0.8}$Mo$_{0.2}$O$_2$/C= 75/25 mass ratio was successfully synthesized as anode catalyst for reformate-fed fuel cells. Studies of the structure, composition and stability, as well as the results of CO$_{ads}$ stripping confirmed that the mixed oxide composite support and the electrocatalyst prepared for this study show the well-documented characteristics of the Pt/Ti$_{1-x}$Mo$_x$O$_2$-C systems and Pt/Ti$_{0.8}$Mo$_{0.2}$O$_2$-C catalyst with enhanced CO tolerance compared to the Pt/C catalyst is suitable for further investigation as an anode in reformate-fed PEM fuel cells.

Loading of 0.85 mgPt/cm^2 was effective to reach a reasonable performance with 25 ppm CO. Higher Pt/support ratio is supposed to be needed to reach high current densities without mass transfer limitations. High pressure operation helped with better CO oxidation leading to higher performance. Since loadings higher than 0.85 mgPt/cm^2 may cause mass transfer issues, higher loadings may be tried with 40 wt.% Pt/ Ti$_{0.8}$Mo$_{0.2}$O$_2$-C support catalyst. Dilution of hydrogen with CO$_2$ and CH$_4$ had limited negative impact on the performance.

Acknowledgement

References

[1] Watanabe M, Motoo S. Electrocatalysis by ad-atoms. Part II. Enhancement of the oxidation of methanol on platinum by ruthenium ad-atoms. J Electroanal Chem 1975;60:267-73.

[2] Gasteiger HA, Markovic NM, Ross PN, Jr. H_2 and CO Electrooxidation on well-characterized Pt, Ru, and Pt-Ru. 1. Rotating Disk Electrode studies of the pure gases including temperature effects. J Phys Chem 1995;99:8290-8301.

[3] Urian RC, Gullá AF, Mukerjee S. Electrocatalysis of reformate tolerance in proton exchange membranes fuel cells: Part I. J Electroanal Chem 2003;554-555:307-24.

[4] Subban C, Zhou Q, Leonard B, Ranjan C, Edvenson HM, DiSalvo FJ, Munie S, Hunting J. Catalyst supports for polymer electrolyte fuel cells. Phil Trans R Soc A 2010;368:3243-53.

[5] Kumar A, Ramani V. $Ta_{0.3}Ti_{0.7}O_2$ Electrocatalyst supports exhibit exceptional electrochemical stability. J Electrochem Soc 2013;160:F1207-15.

[6] Huang SY, Ganesan P, Popov BN. Electrocatalytic activity and stability of niobium-doped titanium oxide supported platinum catalyst for polymer electrolyte membrane fuel cells. Appl Catal B: Environ 2010;96:224-31.

[7] Gao Y, Hou M, Shao Z, Zhang C, Qin X, Yi B. Preparation and characterization of $Ti_{0.7}Sn_{0.3}O_2$ as catalyst support for oxygen reduction reaction. J Energy Chem 2014;23:331-7.

[8] Subban CV, Zhou Q, Hu A, Moylan TE, Wagner FT, DiSalvo FJ. Sol-gel synthesis, electrochemical characterization, and stability testing of $Ti_{0.7}W_{0.3}O_2$ nanoparticles for catalyst support applications in Proton-Exchange Membrane Fuel Cells. J Am Chem Soc 2010;132:17531-6.

[9] Nagel T, Bogolowski N, Samjeske G, Baltruschat H. On the effect of tungsten on CO oxidation at Pt electrodes. J Solid State Electrochem 2003;7:614-8.

[10] Massong H, Wang H, Samjeské G, Baltruschat H. The co-catalytic effect of Sn, Ru and Mo decorating steps of Pt(111) vicinal electrode surfaces on the oxidation of CO. Electrochim Acta 2000;46:701-7.

[11] Wang D, Subban CV, Wang H, Rus E, DiSalvo FJ, Abruña HD (2010) Highly stable and CO-tolerant $Pt/Ti_{0.7}W_{0.3}O_2$ electrocatalyst for Proton-Exchange Membrane Fuel Cells. J Am Chem Soc 132:10218-20.

[12] Grgur BN, Markovic NM, Ross PN. Electrooxidation of H_2, CO, and H_2/CO mixtures on a well-characterized $Pt_{70}Mo_{30}$ bulk alloy electrode. J Phys Chem B 1998;102:2494-501.

[13] Bang JH, Kim H. CO-tolerant PtMo/C fuel cell catalyst for H_2 oxidation. Bull Korean Chem Soc 2011;32(10):3660-3665.

[14] Zeng J, Lee JY. Ruthenium-free, carbon-supported cobalt and tungsten containing binary & ternary Pt catalysts for the anodes of direct methanol fuel cells. Int J Hydrogen Energy 2007;32:4389-96.

[15] Hu JE, Liu Z, Eichhorn BW, Jackson GS. CO tolerance of nano-architectured Pt-Mo anode electrocatalysts for PEM fuel cells. Int J Hydrogen Energy 2012;37:11268-75.

[16] Nguyen TT, Ho VTT, Pan CJ, Liu JY, Chou HL, Rick J, Su WN, Hwang BJ. Synthesis of $Ti_{0.7}Mo_{0.3}O_2$ supported- Pt nanodendrites and their catalytic activity and stability for oxygen reduction reaction. Appl. Catal. B-Environ 2014;154-155:183-9.

[17] Ho VTT, Pan CJ, Rick J, Su WN, Hwang BJ. Nanostructured $Ti_{0.7}Mo_{0.3}O_2$ support enhances electron transfer to Pt: High-performance catalyst for oxygen reduction reaction. J Am Chem Soc 2011;133:11716-24.

[18] Xu T, Zhang H, Zhong H, Ma Y, Jin H, Zhang Y. Improved stability of TiO_2 modified $Ru_{85}Se_{15}$/C electrocatalyst for proton exchange membrane fuel cells. J Power Sources 2010;195:8075-79.

[19] Vass Á, Borbáth I, Pászti Z, Bakos I, Sajó IE, Németh P, Tompos A. Effect of Mo incorporation on electrocatalytic performance of Ti-Mo mixed oxide-carbon composite supported Pt electrocatalysts. React Kinet Mech Cat 2017;121:141-60.

[20] Vass Á, Borbáth I, Bakos I, Pászti Z, Sáfrán Gy, Tompos A. Stability issues of CO tolerant Pt-based electrocatalysts for polymer electrolyte membrane fuel cells: comparison of $Pt/Ti_{0.8}Mo_{0.2}O_2$-C with PtRu/C. React Kinet Mech Cat 2019;126:679-99.

[21] Vass Á, Borbáth I, Bakos I, Pászti Z, Sajó IE, Tompos A. Novel Pt electrocatalysts: multifunctional composite supports for enhanced corrosion resistance and improved CO tolerance. Top Catal 2018;61:1300-12.

[22] Gubán D, Tompos A, Bakos I, Vass Á, Pászti Z, Szabó EG, Sajó IE, Borbáth I. Preparation of CO-tolerant anode electrocatalysts for polymer electrolyte membrane fuel cells. Int J Hydrogen Energy 2017;42:13741-53.

[23] Bakos I, Borbáth I, Vass Á, Pászti Z, Tompos A. Design and investigation of molybdenum modified platinum surfaces for modeling of CO tolerant electrocatalysts. Top Catal 2018;61:1385-95.

[24] Profatilova I, Jacques PA, Escribano S. Evaluation of parameters accelerating the aging of PEMFCs operating under reformate containing carbon monoxide. J Electrochem Soc 2018;165(6):F3251-60.

[25] Ordóñez LC, Roquero P, Sebastian PJ, Ramírez J. CO oxidation on carbon-supported PtMo electrocatalysts: Effect of the platinum particle size. Int J Hydrogen Energy 2007;32:3147-53.

[26] He CZ, Kunz HR, Fenton JM. Evaluation of platinum-based catalysts for methanol electrooxidation in phosphoric-acid electrolyte. J Electrochem Soc 1997;144:970-9.

[27] Martinez-Huerta MV, Rodriguez JL, Tsiouvaras N, Pena MA, Fierro JLG, Pastor E. Novel synthesis method of CO-tolerant $PtRu-MoO_x$ nanoparticles: structural characteristics and performance for methanol electrooxidation. Chemistry of Materials 2008;20:4249-59.

[28] Mukerjee S, Urian RC. Bifunctionality in Pt alloy nanocluster electrocatalysts for enhanced methanol oxidation and CO tolerance in PEM fuel cells: electrochemical and in situ synchrotron spectroscopy. Electrochim Acta 2002;47:3219-31.

[29] Zhou ZH, Li WS, Fu Z, Xiang XD. Carbon nanotube-supported $Pt-H_xMoO_3$ as electrocatalyst for methanol oxidation. Int J Hydrogen Energy 2010;35:936-41.

[30] Zhang Z, Liu J, Gu J, Su L, Cheng L. An overview of metal oxide materials as electrocatalysts and supports for polymer electrolyte fuel cells. Energy Environ Sc. 2014;7:2535-58.

[31] Ordóñez LC, Roquero P, Ramírez J, Sebastian PJ (2016) Methanol Electro-Oxidation on Bimetallic PtMo/C Catalysts and Pt/C-Mo/C Mechanical Mixtures. Int J Electrochem Sci 11:5364-79.

[32] Justin P, Rao GR. Methanol oxidation on MoO_3 promoted Pt/C electrocatalyst. Int J Hydrogen Energy 2011;36:5875-84.

[33] Alcaide F, Álvarez G, Tsiouvaras N, Pena MA, Fierro JLG, Martínez-Huerta MV. Electrooxidation of H_2/CO on carbon-supported $PtRu-MoO_x$ nanoparticles for polymer electrolyte fuel cells. Int J Hydrogen Energy 2011;36:14590-8.

[34] Pereira LGS, Paganin VA, Ticianelli EA. Investigation of the CO tolerance mechanism at several Pt-based bimetallic anode electrocatalysts in a PEM fuel cell. Electrochim Acta 2009;54:1992-8.

[35] Mayrhofer KJJ, Hartl K, Juhart V, Arenz M. Degradation of carbon-supported Pt bimetallic nanoparticles by surface segregation. J Am Chem Soc 2009;131:16348-49.

[36] Lebedeva NP, Janssen GJM. On the preparation and stability of bimetallic PtMo/C anodes for proton-exchange membrane fuel cells. Electrochim Acta 2005;51:29-40.

[37] Micoud F, Maillard F, Gourgaud A, Chatenet M. Unique CO-tolerance of $Pt-WO_x$ materials. Electrochem Commun 2009;11:651-4.

[38] Bauer A, Song C, Ignaszak A, Hui R, Zhang J, Chevallier L, Jones D, Roziére J. Improved stability of mesoporous carbon fuel cell catalyst support through incorporation of TiO_2. Electrochim Acta 2010;55:8365-70.

[39] Lv Q, Yin M, Zhao X, Li C, Liu C, Xing W. Promotion effect of TiO_2 on catalytic activity and stability of Pt catalyst for electrooxidation of methanol. J Power Sources 2012;218:93-9.

[40] Esfahani RAM, Vankova SK, Monteverde Videla AHA, Specchia S. Innovative carbon-free low content Pt catalyst supported on Mo-doped titanium suboxide (Ti_3O_5-Mo) for stable and durable oxygen reduction reaction. Appl Catal B-Environ 2017;201:419-29.